JACS
JOURNAL OF THE AMERICAN CHEMICAL SOCIETY

ARTICLE

pubs.acs.org/JACS

Tracking of the Nuclear Wavepacket Motion in Cyanine Photoisomerization by Ultrafast Pump−Dump−Probe Spectroscopy

Zhengrong Wei, Takumi Nakamura, Satoshi Takeuchi, and Tahei Tahara*

Molecular Spectroscopy Laboratory, Advanced Science Institute (ASI), RIKEN, 2-1 Hirosawa, Wako 351-0198, Japan

ABSTRACT: Understanding ultrafast reactions, which proceed on a time scale of nuclear motions, requires a quantitative characterization of the structural dynamics. To track such structural changes with time, we studied a nuclear wavepacket motion in photoisomerization of a prototype cyanine dye, 1,1′-diethyl-4,4′-cyanine, by ultrafast pump−dump−probe measurements in solution. The temporal evolution of wavepacket motion was examined by monitoring the efficiency of stimulated emission dumping, which was obtained from the recovery of a ground-state bleaching signal. The dump efficiency versus pump−dump delay exhibited a finite rise time, and it became longer (97 fs → 330 fs → 390 fs) as the dump pulse was tuned to longer wavelengths (690 nm → 950 nm → 1200 nm). This result demonstrates a continuous migration of the leading edge of the wavepacket on the excited-state potential from the Franck−Condon region toward the potential minimum. A slowly decaying feature of the dump efficiency indicated a considerable broadening of the wavepacket over a wide range of the potential, which results in the spread of a population distribution on the flat S_1 potential energy surface. The rapid migration as well as broadening of the wavepacket manifests a continuous nature of the structural dynamics and provides an intuitive visualization of this ultrafast reaction. We also discussed experimental strategies to evaluate reliable dump efficiencies separately from other ultrafast processes and showed a high capability and possibility of the pump−dump−probe method for spectroscopic investigation of unexplored potential regions such as conical intersections.

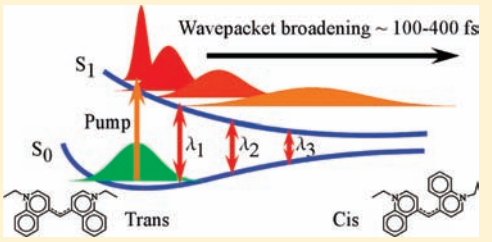

INTRODUCTION

In ordinary "slow" chemical reactions, the well-defined reactant and product are separated by a finite energy barrier, and hence only those reactant molecules that acquire high enough thermal energy can surmount the barrier and are converted to the product. The reactant molecule spends almost the whole time to prepare energy to climb up the barrier, which results in a low reaction rate. In ultrafast photochemical reactions, in contrast, the initial reactant excited state is generated by photoexcitation at the potential region having no substantial energy barrier or even the region that has a substantial slope. Accordingly, each atom of the molecule suddenly feels a force to be displaced upon photoexcitation, inducing rapid structural evolution toward the product. Therefore, ultrafast reactions often proceed with unrestricted continuous structural changes on a time scale comparable to the nuclear motions.

The dynamics of such ultrafast reactions can only poorly be described by conventional population kinetics between the reactant and product. Instead, the description by a nuclear wavepacket is considered highly suitable, because not only the continuous structural change but also structural distribution can intrinsically be well described. The wavepacket concept was introduced to account for electronic and Raman spectra of molecules through initial wavepacket motion along the relevant potential energy surface (PES).[1] Since then, the wavepacket motion has been widely used to describe ultrafast processes, such as photodissociation,[2,3] photoisomerization,[4] proton transfer,[5] quantum control,[6] and so on. The dynamics of these barrierless ultrafast reactions can be depicted as a continuous motion of the wavepacket on a monotonously sloping PES along the reaction coordinate. However, although this wavepacket motion provides an intuitive picture of the dynamics of ultrafast reactions, in reality, we only have very limited knowledge on how the wavepacket evolves on the PES. As a result, it is still a challenging task to experimentally achieve real-time tracking of the wavepacket running on a reactive potential surface through spectroscopic signals and associate them with the reaction dynamics at the molecular level.

Most simply, the wavepacket motion in the S_1 state can be followed by measuring temporal spectral shifts of the fluorescence, because the fluorescence peak wavelength corresponds to the $S_1 \rightarrow S_0$ transition energy at each moment and continuously changes as the wavepacket migrates on the excited-state PES. Fluorescence up-conversion studies of such spectral shifts were reported for ultrafast photoisomerization of a cyanine dye, 1,1′-diethyl-4,4′-cyanine (1144C), as well as for excited-state dynamics of dGMP.[7,8] However, the spontaneous emission probability shows a cubic dependence on the photon energy, and hence the up-conversion measurement becomes harder and harder in the longer wavelength region. This drawback in sensitivity can be partially solved by monitoring the $S_1 \rightarrow S_0$ transition intensity as a stimulated emission signal in the transient absorption experiments,[9,10] although the stimulated emission signal is often contaminated by spectral overlap with other absorption bands.

Received: November 29, 2010
Published: April 22, 2011

dx.doi.org/10.1021/ja110716b | J. Am. Chem. Soc. 2011, 133, 8205–8210

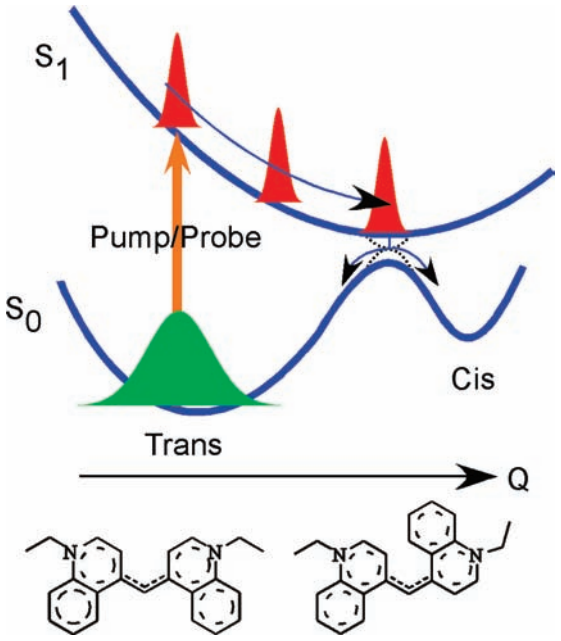

Figure 1. Simplified model potentials and reaction scheme for photoisomerization of 1144C.

The excited-state wavepacket motion can be explored sensitively and selectively by introducing an additional pulse ("dump" pulse) to ordinary pump−probe spectroscopy, which is called pump−dump−probe spectroscopy.[11−14] In this method, the pump pulse generates a wavepacket in the Franck−Condon region of the S_1 PES. After a certain delay, a dump pulse, which is resonant with the $S_1 \rightarrow S_0$ transition, is introduced. The dump pulse drives a fraction of the S_1 state back to the S_0 state by the stimulated emission transition. This increase of the S_0 population induced by the dump pulse can be monitored by the probe pulse as additional recovery of the S_0 bleaching, so that we can "extract" the $S_1 \rightarrow S_0$ dumping transition selectively with a minimum possible contribution from the $S_n \leftarrow S_1$ transition. As is readily understood, the dump process occurs most efficiently when the dump photon energy matches the $S_1 \rightarrow S_0$ transition energy. This means that the pump−dump−probe spectroscopy can tell us when the wavepacket reaches the PES region that corresponds to a given S_1-S_0 energy. This information is crucial for quantitative characterization of the wavepacket motion and the shape of the relevant PES. Furthermore, the pump−dump−probe spectroscopy is advantageous over conventional methods, because it enables us to access the PES region with a small S_1-S_0 gap, such as a vicinity of the conical intersection,[10,15] by using a long-wavelength dump pulse.

In this Article, we report our ultrafast pump−dump−probe study of the wavepacket motion, by taking photoisomerization of a cyanine dye (1144C) in solution as a sample. This molecule is known as a prototypical system showing a barrierless structural evolution along the isomerization coordinate.[7,16−19] As shown in Figure 1, the S_1 population, or wavepacket, is generated at the Franck−Condon region by photoexcitation of the trans form, and then it is supposed to migrate rapidly toward the S_1 potential minimum on a femtosecond time scale. The S_1 state returns to the S_0 state through the "funnel" of S_1 PES (e.g., the conical intersection[20]) with a 7 ps time constant, being branched into the trans or the cis (product) form. Because of the simple reaction scheme, this molecule serves as an ideal model system for quantitative

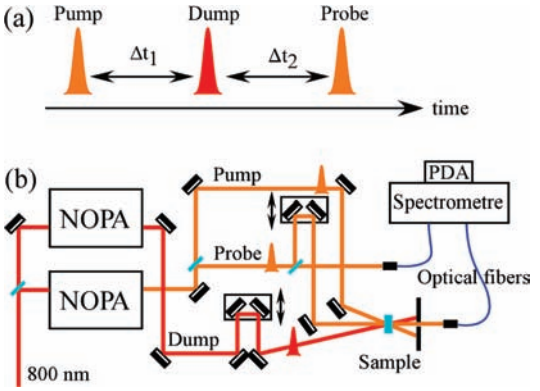

Figure 2. (a) Time sequence of the pump, dump, and probe pulses. (b) Experimental setup for the pump−dump−probe experiment.

studies of the wavepacket motion on the reactive PES. We carried out pump−dump−probe experiments with three different dump wavelengths and found that the dump efficiency showed a dump-wavelength-dependent rise, reflecting different arrival times of the wavepacket at each region of PES. On the basis of the dump efficiency evaluated, we quantitatively characterize the motion and distribution of the S_1 wavepacket in this ultrafast photoisomerization.

EXPERIMENTAL SECTION

The pump−dump−probe measurement was carried out by using a setup that is based on two homemade noncollinear optical parametric amplifiers (NOPA), as shown in Figure 2.[5,21] Briefly, a femtosecond modelocked Ti:sapphire oscillator (Mira-900F, Coherent) provided a train of 800 nm pulses with 0.6 W average power. The oscillator output was used to seed a regenerative amplifier (Legend Elite, Coherent) that produces 80 fs, 1 mJ pulses with a 1 kHz repetition rate. This amplified fundamental pulse was divided into two, and they were used to drive the two NOPAs. The output of the first NOPA (~15 fs, 580 nm) was divided into three, and they served as pump, probe, and reference pulses, respectively. The second NOPA was tuned to 690, 950, or 1200 nm and provided a dump pulse (~20 fs) in the near-infrared region. The pump, dump, and probe pulses were focused together into a thin-film like jet stream of the sample solution (50 μm thickness) after timing adjustments by mechanical stages. The polarization of the pump and dump pulses were set at magic angle (54.7°) with respect to the probe polarization. The probe pulse passing through the sample and the reference pulse were spectrally analyzed by a spectrograph (iHR-320, Horiba), and their spectra of each laser shot were detected by a pair of photodiode arrays (S3904-512Q, Hamamatsu). The pump and dump pulses were separately chopped to evaluate the pump-induced and/or dump-induced absorbance change. This data acquisition as well as delay stages were controlled by a homemade program written on commercial software (IGOR Pro, Wave Metrics). The fwhm values of the pump−probe and pump−dump cross correlation traces were ~23 and ~40 fs, respectively. As shown in Figure 2a, we represent the pump−dump and dump−probe intervals by Δt_1 and Δt_2 times, respectively, hereafter.

1,1′-Diethyl-4,4′-cyanine iodide was purchased from Aldrich, and it was recrystallized from ethanol. Ethylene glycol (99.5%, Wako) was used as received. The 1144C iodide was dissolved in ethylene glycol in the experiments, and 1144C exists as a cation in the sample solution. We used a fresh solution with an optical density of approximately 0.3 at 580 nm for the 50 μm path length.

UV−visible absorption spectra were measured by a commercial spectrometer (U3310, Hitachi). Steady-state fluorescence spectra were

dx.doi.org/10.1021/ja110716b | J. Am. Chem. Soc. 2011, 133, 8205–8210

measured by a spectrograph coupled with a CCD camera. The fluorescence spectra were corrected for spectral sensitivity of the instrument by using 4-dimethylamino-4′-nitrostilbene in *o*-dichlorobenzene as a standard (600−950 nm).[22]

RESULTS AND DISCUSSION

The cyanine dye 1144C in ethylene glycol shows a strong absorption band due to the $S_1 \leftarrow S_0$ transition around 594 nm (Figure 3, black curve). We used a pair of pump and probe pulses that are resonant with this absorption and measured a time-resolved absorption spectrum at a 1 ps pump−probe delay ($\Delta t_1 + \Delta t_2 = 1$ ps) within a spectral coverage of the probe pulse (550−610 nm). As shown by a blue curve in Figure 4a, the observed transient spectrum exhibits a negative band that is assignable to depletion of the ground-state population (S_0 bleaching), as well as occupation of the Franck−Condon state. Temporal behavior of this bleaching signal at 600 nm is depicted in blue in Figure 4b. We found that the observed transient can be well reproduced by a three-exponential function with time constants of τ_1 = 100 fs, τ_2 = 7 ps, and τ_3 = 17 ps. Considering the relaxation scheme in Figure 1, the τ_1 component is ascribable to the initial escape of the S_1 population from the Franck−Condon region,[18] which is closely related to the wavepacket motion on the S_1 PES that we investigate in this work. A similar dynamics was also observed by transient grating measurements.[18] The τ_2 value is equal to a decay time constant of the S_1 absorption observed around 500 nm (not shown). Therefore, it can be attributed to the lifetime of the S_1 state, that is, the time constant of the $S_1 \rightarrow S_0$ internal conversion. This S_1 lifetime (7 ps) agrees reasonably well with the literature values measured in various solvents (τ_2 is solvent-dependent).[23] The τ_3 component is specifically observed in the S_0 bleaching signal, and its origin has not yet fully been clarified. Nevertheless, we consider that it is, at least partially, due to a vibrational cooling process of the S_0 molecule after the internal conversion.[24] Thus, the present pump−probe data (drawn in blue) in Figure 4 represent how the S_1 molecule comes back to the S_0 state.

To examine the wavepacket motion on the S_1 PES, we introduced a dump pulse that is tuned to 950 nm within a spectral region of the $S_1 \rightarrow S_0$ fluorescence (or stimulated emission), as shown in Figure 3. We measured a transient absorption spectrum with presence of the dump pulse ("pump−dump−probe" signal) for a pump−dump interval of Δt_1 = 0.5 ps and a pump−probe delay of 1 ps ($\Delta t_1 + \Delta t_2$). As shown by a red curve in Figure 4a, the transient absorption signal is substantially decreased, as compared to the case without the dump pulse. This observation clearly indicates that a portion of the S_1 population is driven back to the S_0 state by the stimulated emission process induced by the dump pulse. A prompt decrease of the bleaching signal at Δt_1 = 0.5 ps can also be recognized in the temporal trace in Figure 4b.

For quantitative evaluation of the dump effect, we defined the following dump efficiency (η) by using the transient absorption signals with (ΔA_{on}) and without (ΔA_{off}) the dump pulse:

$$\eta = \left| \frac{\Delta A_{on} - \Delta A_{off}}{\Delta A_{off}} \right| = \left| \frac{\Delta A_{diff}}{\Delta A_{off}} \right| \quad (1)$$

where $\Delta A_{diff} = \Delta A_{on} - \Delta A_{off}$ is a difference signal. This dump efficiency represents how much fraction of the S_1 population is transferred back to the ground state by the dump pulse.

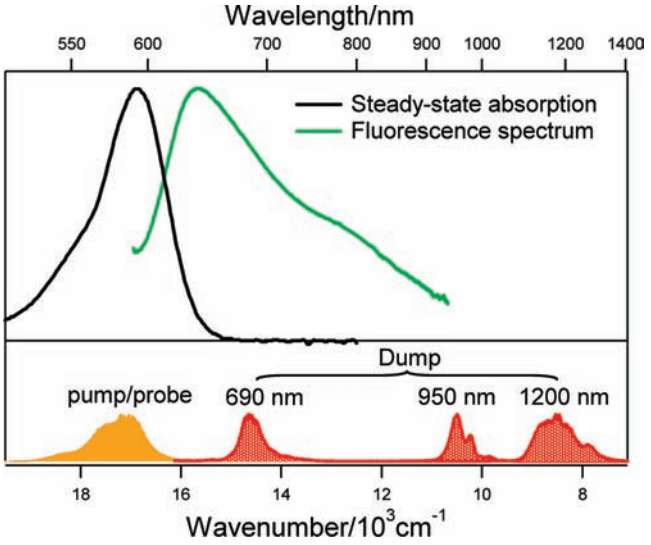

Figure 3. Steady-state absorption and emission spectra of 1144C in ethylene glycol, together with spectra of the pump/probe and dump pulses used in the pump−dump−probe experiments.

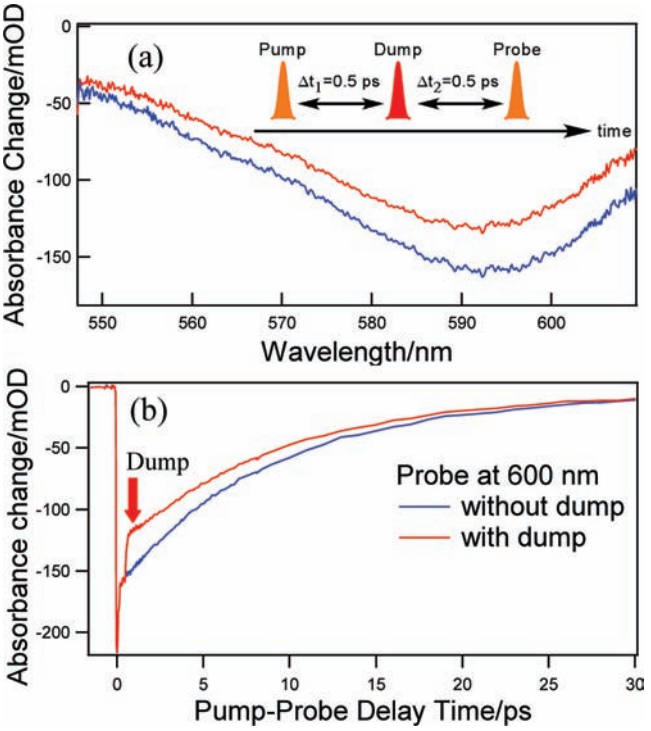

Figure 4. (a) Transient absorption spectra of 1144C in ethylene glycol measured with (red) and without (blue) the 950 nm dump pulse. Both the pump−dump interval and the dump−probe interval were set at 0.5 ps. (b) Temporal changes of the transient absorption signals measured with (red) and without (blue) the dump pulse.

Undumped S_1 molecules, which remain after the dump pulse, are expected to behave in the same manner just as the S_1 molecules observed in the absence of the dump pulse. Therefore, simply considering, the dump efficiency is expected to be constant for a given Δt_1 time, regardless of when and at which wavelength it is evaluated. However, we found that the "apparent"

dx.doi.org/10.1021/ja110716b |*J. Am. Chem. Soc.* 2011, 133, 8205–8210

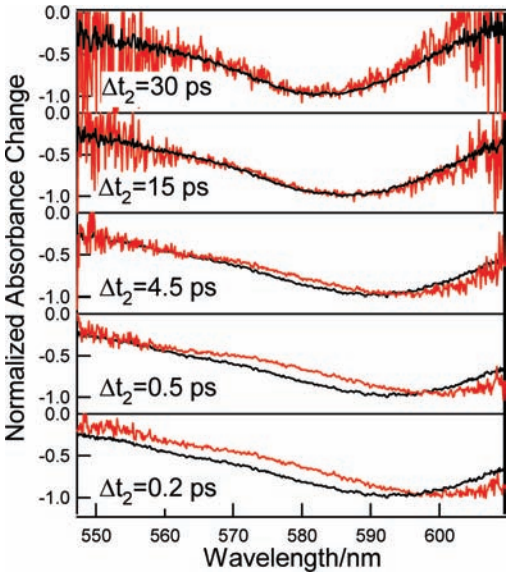

Figure 5. Comparison between the dump-induced absorption difference spectrum (ΔA_{diff}, red) and the ordinary transient absorption spectrum without the dump (ΔA_{off}, black). The dump−probe delays are Δt_2 = 0.2, 0.5, 4.5, 15, and 30 ps (Δt_1 = 0.5 ps). The sign of the ΔA_{diff} spectrum was inverted, and the amplitudes of the two spectra were normalized.

dump efficiency varies depending on the Δt_2 time as well as the wavelength. In fact, we recognize a noticeable spectral difference between the (normalized) ΔA_{diff} and ΔA_{off} spectra especially for early Δt_2 times (Figure 5), which results in different η values calculated with eq 1. This implies that additional dump-induced processes also contribute to the signal. As shown in Figure 5, the spectral difference becomes smaller on the several-picoseconds time scale and essentially vanishes by 15 ps. Therefore, we conclude that we need to wait for at least Δt_2 = 15 ps after the dump pulse to evaluate a dump efficiency, which is independent of the wavelength as well as the Δt_2 time. In other words, waiting for Δt_2 = 15 ps gives a true dump efficiency that purely reflects the $S_1 \rightarrow S_0$ population transfer that is induced by the dump pulse. We note that the spectral evolution shown in Figure 5 highly likely arises from vibrationally hot S_0 molecules generated by the dump pulse. A red-shifted $S_1 \leftarrow S_0$ absorption expected for such hot S_0 molecules is fully consistent with the observed red-shift of ΔA_{diff} as compared to ΔA_{off}. In addition, the red shift disappears with time similar to a typical vibrational cooling time in organic solvents (~10 ps).[25,26]

On the basis of the above discussion, we fixed the Δt_2 time at 15 ps and measured the transient absorption with scanning the Δt_1 time to evaluate the (true) dump efficiency as a function of Δt_1. Figure 6b shows the Δt_1 dependence of the dump efficiency evaluated at 580 nm for the dump wavelength of 950 nm. Interestingly, the dump efficiency does not rise instantaneously but shows a finite rise time of 330 fs. This finite rise time reflects the wavepacket motion on the S_1 PES. As illustrated in Figure 1, the S_1 PES is supposed to exhibit a downward slope from the Franck−Condon region toward the potential minimum, whereas the S_0 PES exhibits an upward slope, along the isomerization coordinate of the 1144C molecule. As a result, the S_1-S_0 transition energy is the largest at the Franck−Condon structure, corresponding to the absorption peak wavelength (~594 nm, 16 835 cm^{-1}), and then it gradually decreases as the wavepacket

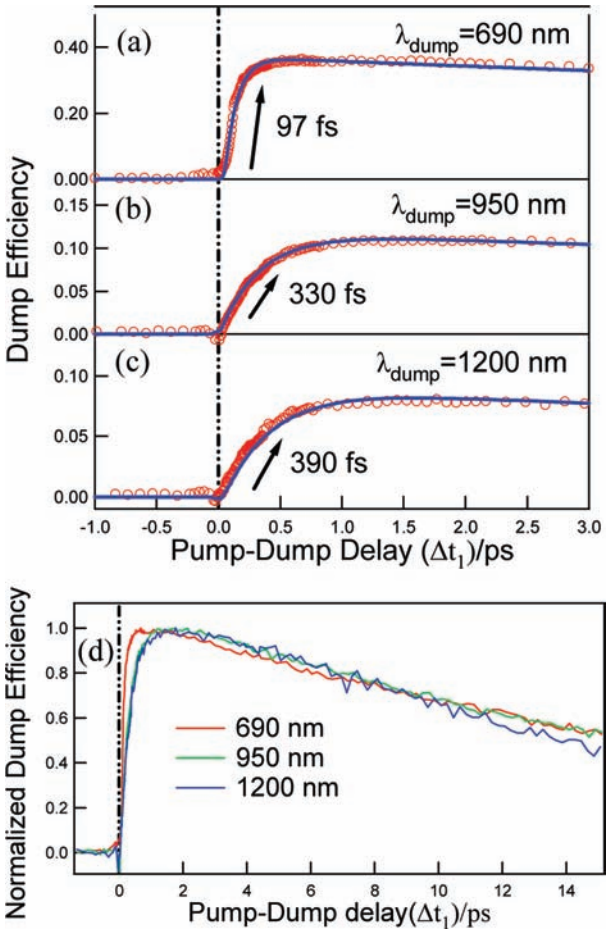

Figure 6. Plots of the dump efficiency as a function of the pump−dump delay (Δt_2 = 20, 15, and 10 ps for 690, 950, and 1200 nm dump pulses, respectively). (a−c) The dump efficiency in the early time region obtained with the dump wavelength of 690, 950, and 1200 nm. The dump pulse energies are 1.7 μJ (690 nm), 0.7 μJ (950 nm), and 0.6 μJ (1200 nm). (d) The three dump efficiencies in the late time region.

migrates toward the S_1 potential minimum. This means that the wavepacket can pass through the PES region where the S_1-S_0 transition energy matches the photon energy of the dump pulse (950 nm, 10 526 cm^{-1}). It is readily understood that, if the dump pulse is irradiated just when the wavepacket reaches this PES region, the S_1 population is transferred back to the S_0 state most efficiently. Therefore, the data in Figure 6b demonstrate that the wavepacket needs 330 fs to reach the PES region that is specified by the 950 nm dump pulse.

For fully tracking the wavepacket motion, we also carried out the pump−dump−probe experiments with two other dump wavelengths, 690 and 1200 nm. The "safe" waiting time to avoid the effect of the vibrational cooling was examined in a similar way, and it was determined as Δt_2 = 20 ps (690 nm) and 10 ps (1200 nm). With this fixed Δt_2 time, we obtained the Δt_1 dependence of the dump efficiency, as shown in Figure 6. Similarly to the case of the 950 nm dump, the dump efficiency with the 690 and 1200 nm dump exhibits a finite rise, and the rise time was evaluated as 97 and 390 fs, respectively. As is clearly seen in Figure 6a−c, the rise time of the dump efficiency becomes longer as 97 fs → 330 fs → 390 fs, when the dump photon energy decreases as 14 493 cm^{-1} → 10 526 cm^{-1} → 8333 cm^{-1}. Because

dx.doi.org/10.1021/ja110716b | J. Am. Chem. Soc. 2011, 133, 8205–8210

the smaller photon energy can be resonant with the $S_1 \rightarrow S_0$ transition at the PES region more distant from the Franck–Condon region, the present result experimentally demonstrates that the wavepacket needs a longer time to reach the PES region more far away from the Franck–Condon region. These data experimentally reveal a continuous motion of the wavepacket on the S_1 PES, which corresponds to a gradual structural evolution of the reacting excited-state molecule. Previously, the wavepacket motion in photoisomerization of 1144C was investigated by fluorescence up-conversion,[7] and a finite rise time of the fluorescence was observed in the long wavelength region, which is consistent with our result. However, the observation wavelength was limited to 900 nm because the probability of the spontaneous emission becomes smaller in the longer wavelength region. As compared to the fluorescence up-conversion, the present pump–dump–probe spectroscopy can sensitively detect the wavepacket motion at wavelengths as long as 1200 nm. Dumping at even longer wavelengths is possible in principle, which allows us to explore the PES region closer to the potential minimum. Thus, the pump–dump–probe spectroscopy is a powerful method for quantitative characterization of the wavepacket motion in a wide PES region.

As shown in Figure 6a–c, the dump efficiency does not exhibit a rapid decrease after reaching the maximum even with the shortest dump wavelength. As discussed above, the dump wavelength of 690 nm corresponds to the S_1 PES region that is closer to the Franck–Condon region as compared to the other two dump wavelengths. Simply considering, if the wavepacket passes through and goes out of the PES region selected by the dump wavelength, the dump efficiency is expected to vanish because we do not have S_1 population that can be resonantly dumped to the S_0 state. The present result shown in Figure 6 is obviously different from this simple expectation and indicates that the wavepacket becomes broader with a substantial amplitude spread over a wide range of the S_1 PES. Because the coherence of nuclear motion is lost in a few picoseconds, the process observed in the present experiment highly likely corresponds to the broadening of the coherent wavepacket, which results in incoherent populational distribution widely spread on the flat S_1 PES. We consider that the rise of the dump efficiency corresponds to the leading edge of the wavepacket in this broadening process. It is noteworthy that the rapid spread of the wavepacket distribution along the reaction coordinate was theoretically demonstrated using semiclassical dynamics simulations as well as recent quantum dynamics simulations for a model cyanine dye, trimethine[27,28] (vide infra).

Last, we mention the temporal behavior of the dump efficiency in the late time region. As shown in Figure 6d, all of the dump efficiencies obtained with the three dump wavelengths exhibit a slow decay with a time constant of ~20 ps. We note that, in this experiment, the dump efficiency is affected by the formation of the cis product, which is formed following the $S_1 \rightarrow S_0$ internal conversion with a time constant of 7 ps. The formation of the cis product contributes to the bleaching signal we observed, but it cannot be dumped, thereby making the dump efficiency smaller. This effect can be more significant at late times when the cis product is more populated and the S_1 state is less populated. Consequently, the formation of the cis product makes the dump efficiency decay slowly on a picosecond time scale, even when the real dump efficiency for the S_1 population is constant over the time. We consider that the slow decay in Figure 6d, at least partially, reflects the formation of the cis product and that the real dump efficiency for the S_1 population should be larger than that observed in the late time region. We also note a possibility that vibrational energy redistribution and/or vibrational cooling on the picosecond time scale might reduce the oscillator strength of the $S_1 \rightarrow S_0$ transition and induce the slow decay of the dump efficiency.

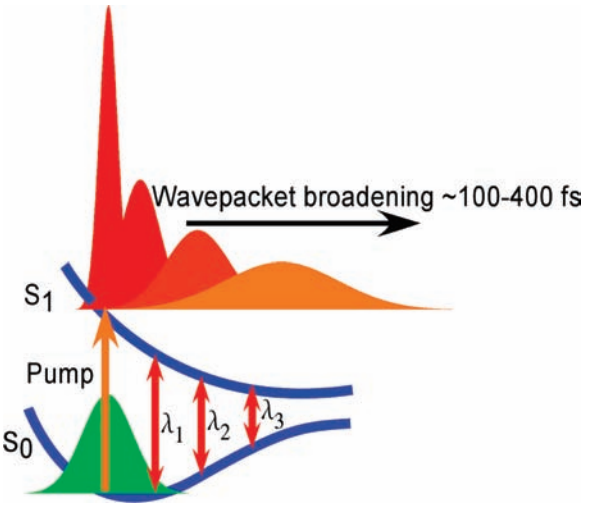

Figure 7. Schematic illustration of the wavepacket motion on the S_1 PES during photoisomerization of 1144C, which is obtained by the present pump–dump–probe spectroscopy.

Figure 7 illustrates a schematic picture of the wavepacket motion in photoisomerization of a prototype cyanine dye, 1144C, which was obtained by the present pump–dump–probe experiment. The photoexcitation of the visible absorption band at 580 nm generates S_1 molecules having the Franck–Condon structure. Time evolution of the S_1 molecules, including the structural change, can be better described by a nuclear wavepacket motion rather than a conventional kinetic population model. We monitored the temporal evolution of the wavepacket through the efficiency of stimulated emission dumping, which was evaluated from the S_0 bleaching recovery. From the finite rise times of the dump efficiency obtained with three different dump wavelengths, we concluded that the leading edge of the wavepacket migrates rapidly from the Franck–Condon region toward the potential minimum on the 400 fs time scale. The slowly decaying feature of the dump efficiency revealed a significant broadening of the wavepacket over a wide range of the PES. The fast migration as well as broadening of the wavepacket demonstrates essential features of this ultrafast reaction with unrestricted nuclear motions, corresponding to the continuous structural evolution along the reaction coordinate.

The present pump–dump–probe experiment demonstrated that the migration of the leading edge of the wavepacket is completed on a subpicosecond time scale, which results in a quasi-stationary populational distribution spread over a wide range of the S_1 PES. The following population decay of the S_1 to the S_0 state occurs slowly with a time constant of ~7 ps without substantial change in the character of the quasi-stationary S_1 state (at least from a viewpoint of spectroscopic information). This large separation of the two time scales indicates that the conical intersection (or the conical intersection seam) is not located on the coordinate along which the wavepacket initially spreads, because a typical time of the internal conversion through the conical intersection itself is very short (~100 fs[10,29]).

dx.doi.org/10.1021/ja110716b | J. Am. Chem. Soc. 2011, 133, 8205–8210

Experimentally, we cannot rule out the possibility that the ~7 ps internal conversion occurs around the S_1 potential minimum where S_1 and S_0 potentials are very close but not crossed. However, the separation of the two time scales looks to suggest that a one-dimensional picture, which has most often been used by experimentalists so far, is not sufficient to properly describe the isomerization process of this prototypical cyanine. In fact, recent theoretical studies of a simplified model cyanine (trimethine) concluded that multidimensionality is essential to understand the isomerizaion process occurring in the S_1 state.[19,27,28] Especially, molecular dynamics simulation on the S_1 PES indicated that the relaxation on S_1 PES proceeds in two steps: The wavepacket first spreads very rapidly along the minimum energy path to cover almost all twist angles, and then the molecule slowly "diffuses" toward the conical intersection seam that runs roughly parallel to the minimum energy path. In this regard, the experimental data seem to accord with this two-step picture suggested by the theoretical studies. It may be worth noting that the time scale of the two steps calculated in the theoretical studies is substantially shorter than the corresponding time scale observed for 1144C in the experiment (~400 fs and ~7 ps). It is highly possible that this difference is due to the difference in the size of the molecular system. The quinoline rings are absent in the model cyanine examined in the theoretical studies, and the difference in the π conjugation is expected to substantially change the potential gradient along the minimum energy path on the S_1 PES. It is also natural to think that the second diffusion process toward the conical intersection (seam) takes much longer time in 1144C because of its much larger degree of the vibrational freedom. Therefore, the experimental data look consistent with the theoretical results in essential points.

The pump−dump−probe experiments with various dump wavelengths can, in principle, determine the $S_1 \rightarrow S_0$ transition energy as a function of time. Such information on the transition energy versus time has been translated to the structural dynamics for simple gas-phase molecules, for which the transition energy as a function of nuclear coordinates is accurately known.[3,30] Now, even for condensed-phase molecules, the pump−dump−probe experiments combined with molecular dynamics simulations can lead to a tracking of the structural change directly in the time domain. Thus, the present pump−dump−probe spectroscopy provides a quantitative characterization of the wavepacket motion that intuitively visualizes the continuous structural evolution in ultrafast reactions.

AUTHOR INFORMATION

Corresponding Author
Fax +86-467-4539; E-mail: tahei@riken.jp.

ACKNOWLEDGMENT

This work was supported by a Grant-in-Aid for Scientific Research on Priority Area "Molecular Science for Supra Functional Systems" (No. 19056009) from MEXT and a Grant-in-Aid for Scientific Research (A) (No. 22245005) from JSPS.

REFERENCES

(1) Heller, E. J. *Acc. Chem. Res.* **1981**, *14*, 368.
(2) (a) Rose, T. S.; Rosker, M. J.; Zewail, A. H. *J. Chem. Phys.* **1988**, *88*, 6672. (b) Takeuchi, S.; Tahara, J. *J. Chem. Phys.* **2004**, *120*, 4768.
(3) Williams, S. O.; Imre, D. G. *J. Phys. Chem.* **1988**, *92*, 6648.
(4) (a) Dietzek, B.; Brüggemann, B.; Pascher, T.; Yartsev, A. *Phys. Rev. Lett.* **2006**, *97*, 258301. (b) Ishii, K.; Takeuchi, S.; Tahara, T. *Chem. Phys. Lett.* **2004**, *398*, 400. (c) Takeuchi, S.; Ruhman, S.; Tsuneda, T.; Chiba, M.; Taketsugu, T.; Tahara, T. *Science.* **2008**, *322*, 1073. (d) Ishii, K.; Takeuchi, S.; Tahara, T. *J. Phys. Chem. A* **2008**, *112*, 2219.
(5) Takeuchi, S.; Tahara, T. *J. Phys. Chem. A* **2005**, *109*, 10199.
(6) Tannor, D. J.; Kosloff, R.; Rice, S. A. *J. Chem. Phys.* **1986**, *85*, 5805.
(7) Yartsev, A.; Alvarez, J. L.; Åberg, U.; Sundström, V. *Chem. Phys. Lett.* **1995**, *243*, 281.
(8) Miannay, F. A.; Gustavsson, T.; Banyasz, A.; Markovitsi, D. *J. Phys. Chem. A* **2010**, *114*, 3256.
(9) Dietzek, B.; Yartsev, A.; Tarnovsky, A. N. *J. Phys. Chem. B* **2007**, *111*, 4520.
(10) Polli, D.; Altoè, P.; Weingart, O.; Spillane, K. M.; Manzoni, C.; Brida, D.; Tomasello, G.; Orlandi, G.; Kukura, P.; Mathies, R. A.; Garavelli, M.; Cerullo, G. *Nature* **2010**, *467*, 440.
(11) Bismuth, O.; Komm, P.; Friedman, N.; Eliash, T.; Sheves, M.; Ruhman, S. *J. Phys. Chem. B* **2010**, *114*, 3046.
(12) Kennis, J. T. M.; Larsen, D. S.; van Stokkum, I. H. M.; Vengris, M.; van Thor, J. J.; van Grondelle, R. *Proc. Natl. Acad. Sci. U.S.A.* **2004**, *101*, 17988.
(13) Larsen, D. S.; Vengris, M.; van Stokkum, I. H. M.; van der Horst, M. A.; de Weerd, F. L.; Hellingwerf, K. J.; van Grondelle, R. *Biophys. J.* **2004**, *86*, 2538.
(14) Ruhman, S.; Hou, B. X.; Friedman, N.; Ottolenghi, M.; Sheves, M. *J. Am. Chem. Soc.* **2002**, *124*, 8854.
(15) Lim, J. S.; Kim, S. K. *Nat. Chem.* **2010**, *2*, 627.
(16) Alvarez, J. L.; Yartsev, A.; Åberg, U.; Åkesson, E.; Sundström, V. *J. Phys. Chem. B* **1998**, *102*, 7651.
(17) Dietzek, B.; Pascher, T.; Yartsev, A. *J. Phys. Chem. B* **2007**, *111*, 6034.
(18) Xu, Q. H.; Fleming, G. R. *J. Phys. Chem. A* **2001**, *105*, 10187.
(19) Sanchez-Galvez, A.; Hunt, P.; Robb, M. A.; Olivucci, M.; Vreven, T.; Schlegel, H. B. *J. Am. Chem. Soc.* **2000**, *122*, 2911.
(20) Bernardi, F.; Olivucci, M.; Robb, M. A. *Chem. Soc. Rev.* **1996**, *25*, 321.
(21) Nakamura, T.; Takeuchi, S.; Shibata, M.; Demura, M.; Kandori, H.; Tahara, T. *J. Phys. Chem. B* **2008**, *112*, 12795.
(22) Lakowicz, J. R. *Principles of Fluorescence Spectroscopy*; 3rd ed.; Springer Science+Business Media: New York, 2006.
(23) Åberg, U.; Sundström, V. *Chem. Phys. Lett.* **1991**, *185*, 461.
(24) Iwata, K.; Hamaguchi, H. *J. Phys. Chem. A* **1997**, *101*, 632.
(25) Fujino, T.; Tahara, T. *J. Phys. Chem. A* **2000**, *104*, 4203.
(26) Sarkar, N.; Takeuchi, S.; Tahara, T. *J. Phys. Chem. A* **1999**, *103*, 4808.
(27) Hunt, P. A.; Robb, M. A. *J. Am. Chem. Soc.* **2005**, *127*, 5720.
(28) Allan, C. S. M.; Lasorne, B.; Worth, G. A.; Robb, M. A. *J. Phys. Chem. A* **2010**, *114*, 8713.
(29) Horio, T.; Fuji, T.; Suzuki, Y. I.; Suzuki, T. *J. Am. Chem. Soc.* **2009**, *131*, 10392.
(30) Dantus, M.; Rosker, M. J.; Zewail, A. H. *J. Chem. Phys.* **1987**, *87*, 2395.